



ASSESSING SEISMIC PERFORMANCE OF COMPOSITE (RCS) AND STEEL MOMENT FRAMED BUILDINGS

Sameh S F MEHANNY¹ And Gregory G DEIERLEIN²

SUMMARY

Investigated is the seismic performance of composite special moment frame systems composed of reinforced concrete columns and steel beams. A composite building, designed according to recently proposed seismic design standards, is analysed by static push-over and nonlinear time history analyses under a series of ground motions (two bins of general and near-fault records with forward directivity) at different hazard levels. A new technique is presented by which local seismic damage indices are computed at the structural component level and then integrated through a global frame stability analysis under gravity loads. Stability and drift indices are related to performance levels suggested by codes and to a comparable structural steel moment frame design. Both the steel and RCS frames are shown to consistently exceed the life safety and near collapse performance levels implied by current building codes. Also presented are suggestions for additional ground motion parameters, beyond the standard intensity index of spectral acceleration, that can reduce uncertainties in estimating median response with a limited set of nonlinear time history analyses.

INTRODUCTION

Over the past twenty years, composite moment frame building systems, or so-called RCS frames consisting of reinforced concrete (RC) columns and steel beams, have been used in the US and Japan as a cost-effective alternative to traditional structural steel or RC construction (Griffis 1992). Compared to high-rise steel buildings, RCS systems offer more efficient use of materials, a reduction in total construction time, and the elimination of field welding at beam-column connections. The latter helps avoid fracture problems experienced with welded steel connections that were observed after the Northridge earthquake.

In spite of the advantages of RCS systems, their use in high seismic regions has been constrained by the lack of design information on composite component behavior and inelastic system performance. Accordingly, one goal of this study is to demonstrate the reliable seismic response of RCS frames. This in turn requires modern ways to quantify their performance. Based on a more complete study by Mehanny (1999), the goals of this paper are to (1) review capabilities of models developed by the authors to analyze RCS and steel moment frames, (2) propose damage indices and performance criteria to assess seismic performance of RCS frames under multi-level earthquake hazards, and (3) evaluate the seismic performance implied by building code requirements for RCS frames in the 1997 AISC-Seismic Provisions and the forthcoming International Building Code (IBC) 2000.

ANALYTICAL MODELING TOOLS

DYNAMIX – a program for the DYNAMIC Analysis of MIXed (steel-concrete) structures has been developed through this and previous research with capabilities to perform inelastic static and dynamic analyses of three-dimensional steel and RCS frames (El-Tawil et al. 1996a). Employing a bounding surface stress-resultant plasticity model, inelastic section behavior (i.e., moment-curvature response captured through the bounding surface model) is integrated to simulate overall member response through a flexibility element formulation. The resulting element accounts for the interaction of axial loads and biaxial bending moments in steel, RC, and composite beam-columns, including the effects of spread-of-plasticity, geometric nonlinearities (P- Δ and P- δ),

¹ Graduate Research Assistant, John A. Blume Earthquake Engineering Center, Stanford University, Stanford, CA 94305-4020

² Associate Professor, John A. Blume Earthquake Engineering Center, Stanford University, Stanford, CA 94305-4020

and cyclic stiffness degradation. DYNAMIX also includes models for composite beams, i.e., composite floor decks on steel beams (Mehanny 1999), and composite connections between RC columns and steel beams. The latter account for finite joint size and inelastic panel shear and bearing deformations with cyclic stiffness/strength degradation (El-Tawil et al. 1996b).

SEISMIC DAMAGE INDICES

Damage indices provide criteria to quantify the performance of structural elements, sub-assemblages, and overall system response to a given loading. Aside from their role in relating numerical response quantities to physical damage descriptions, damage indices are necessary to establish structural acceptance criteria at near collapse levels since even today's best analytical models alone cannot faithfully simulate structural collapse under earthquake induced dynamic effects.

A new ductility damage index is introduced, whose chief characteristics are to (1) account for cumulative damage, (2) reflect the temporal effects of loading sequence, and (3) readily accommodate the response of structural components with unsymmetrical behavior, e.g., composite beams. The index is described by the following expression

$$D_{\theta}^{+} = \frac{\left(\theta_p^{+} |_{\text{current PHC}}\right)^{\alpha} + \left(\sum_{i=1}^{n^{+}} \theta_p^{+} |_{\text{FHC},i}\right)^{\beta}}{\left((\theta_f - \theta_y)^{+}\right)^{\alpha} + \left(\sum_{i=1}^{n^{+}} \theta_p^{+} |_{\text{FHC},i}\right)^{\beta}} \quad (1)$$

where inelastic component deformations (expressed symbolically as θ) are distinguished between primary and follower cycles and accumulated over the loading history. Primary Half Cycle (PHC) is the name given to any half cycle with an amplitude that exceeds that in all previous cycles, and Follower Half Cycle (FHC) refers to all subsequent cycles of smaller amplitude. $(\theta_f - \theta_y)^{+}$ is the plastic rotation capacity of the element up to failure under monotonic loading in the positive deformation direction, and α , and β are calibration parameters. A similar damage component D_{θ}^{-} is defined for negative (reverse) deformations, and the two indices, D_{θ}^{+} and D_{θ}^{-} are combined into a single damage index D_{θ} as follows, $D_{\theta} = \sqrt[\gamma]{(D_{\theta}^{+})^{\gamma} + (D_{\theta}^{-})^{\gamma}}$ where γ is a third calibration parameter. Failure is defined when $D_{\theta} \geq 1.0$.

Among major advantages of the proposed index is its dual purpose in capturing both 'peak' and 'cumulative ductility' effects. Generally speaking, the proposed ductility index relates to simpler ductility acceptance criteria used in ATC 40 (Seismic Evaluation and Retrofit of Concrete Buildings) and FEMA 273 (NEHRP Guidelines for the Seismic Rehabilitation of Buildings), but still captures many cumulative effects related to energy measures and further includes loading sequence effects that can be significant in the damage calculation/prediction process. An example relating the computed damage index to corresponding structural damage in an RCS beam-column joint specimen is shown in Fig. 1. The test data shown in this figure are from previous tests of composite RCS connection subassemblies by Kanno and Deierlein (1996).

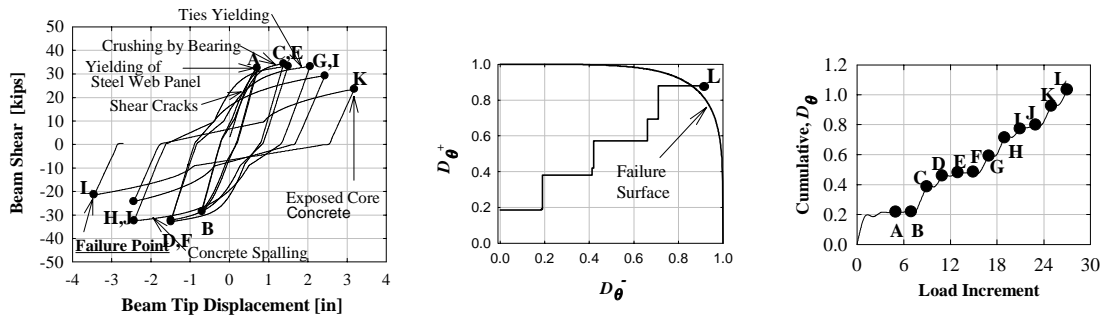


Figure 1. Evolution of damage and damage index in composite beam-column connection.

CASE STUDY BUILDING DESIGNS

The case study building (see structural plan in Fig. 2) is developed according to the general layout of a theme structure proposed as part of the US-Japan program on hybrid structures. It is designed as a 6-story building in high seismic region according to appropriate portions of the following standards: 2000 IBC, AISC Seismic Provisions (1997), and the ASCE Design Guidelines for composite moment connections (ASCE, 1994). Seismic design forces are based on mapped spectral accelerations $S_s=1.5g$ and $S_1=0.72g$, corresponding to the seismic hazard for a 2% in 50 year earthquake. Composite (RCS) and steel framed designs are developed, both employing a space frame configuration where the lateral system consists of seven Special Moment Frames (SMF) in the short direction and four SMFs in the long direction. Member dimensions and reinforcement for the two designs are given in Table 1. Structural steel is A572 Gr. 50 ($F_y = 350$ MPa), reinforcing steel is A706 Gr. 60 ($F_y = 410$ MPa), and concrete has a minimum specified compression strength of $f'_c = 40$ MPa. All SMFs satisfy the minimum strength, stiffness (drift), and strong column-weak beam (SCWB) requirements specified by the IBC 2000. Member sizes in the steel frame were governed nearly exclusively by drift requirements as were the beams in the RCS frame, and reinforced concrete columns in the RCS frame were governed by the SCWB criterion. The fundamental period for the RCS and steel frames spanning in the short direction is $T_1 = 1.25$ seconds. Including the site (soil) response factor in the IBC 2000, the 2% in 50 year spectral coefficient at T_1 , $S_a(T_1) = 0.86g$. The seismic mass (weights) and resulting design base shears for the RCS and steel frames are $W = 5450$ kN and 4780 kN and $V_d/W = 0.12$ and 0.10, respectively.

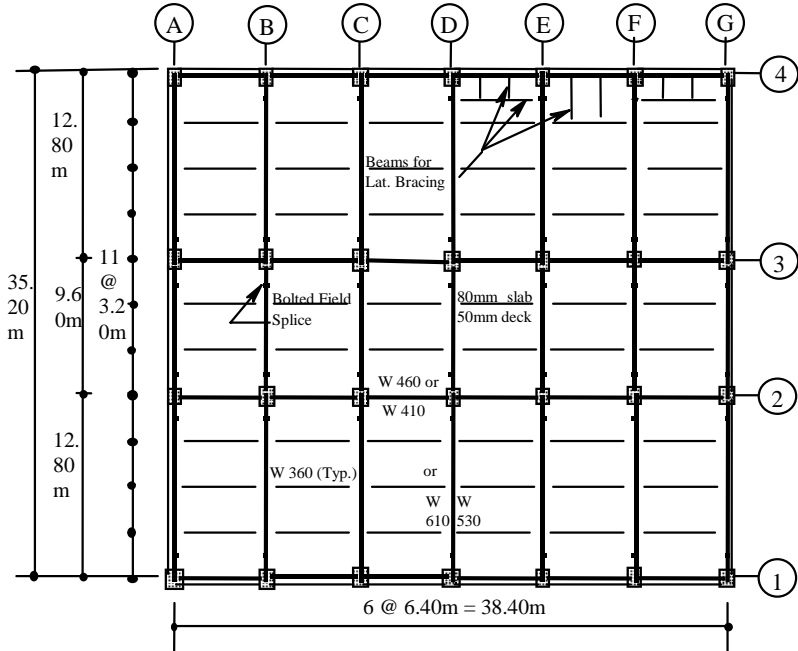


Figure 2. Structural framing plan of typical floor (RCS theme structure).

Table 1 Frame Member Sizes and Dimensions

Floor #	Columns Cross-Sections		Beams Cross-Sections	
	Lines 1 & 4	Lines 2 & 3	Lines A – G	Lines 1 – 4
RCS Building				
1 - 4	650x650 mm 12-29mm bars	650x650 mm 12-32mm bars	W 610x101	W 460x89
5 - 6	600x600 mm 12-25mm bars	600x600 mm 12-29mm bars	W 530x92	W 410x60
STEEL Building				
1 - 4	W 360x314	W 360x314	W 610x101	W 460x89
5 - 6	W 360x262	W 360x262	W 530x92	W 410x60

STATIC PUSH-OVER ANALYSIS AND OVERSTRENGTH VALUES

A two-dimensional static pushover analysis with geometric nonlinearity ($P-\Delta$ effects) is performed on RCS and STEEL frames in the short three-bay framing direction using the IBC 2000 equivalent lateral force distribution. The base shear/weight ratio versus roof drift ratio is shown in Fig. 3 where the full dead load and 25% of the live load were applied prior to ramping up the lateral loading. The resulting static lateral overstrength, $\Omega = V_u/V_d$, is about 3.9 and 6.0 for RCS and STEEL frames, respectively. These analyses reflect the following sources of overstrength: (1) expected versus minimum specified material strengths, (2) minimum stiffness (*drift*) criteria, (3) structural redundancy, (4) SCWB criterion, and (5) discrete member sizing. The particularly large overstrength in the steel frame is attributed to the minimum stiffness (*drift*) requirements and the use of a distributed space frame with relatively shallow members. One can show, for example, that for stiffness controlled designs, the shallower beams in the space frames will result in higher seismic overstrength than with deeper beams commonly found in perimeter frame systems.

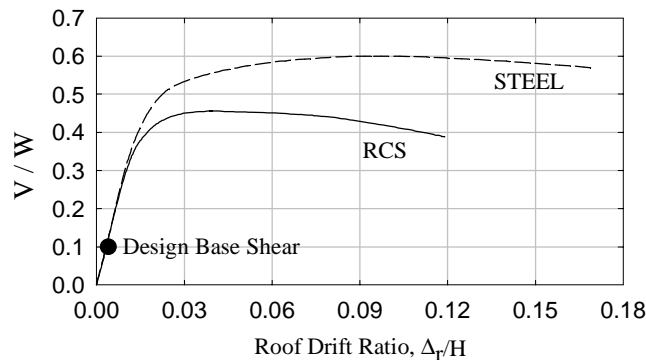


Figure 3. Static push-over curves - IBC 2000 load pattern.

TIME HISTORY ANALYSES AND PERFORMANCE ASSESSMENT

Seismic performance is assessed through nonlinear time history analyses using two sets of acceleration records. One set is comprised of eight “general” records, characterized by magnitude/distance measures of $M = 6.9$ to 8 and $R = 8.5$ to 66 km, and the second set includes eight “near-fault” records exhibiting forward directivity effects with $M = 6.7$ to 7 , $R = 1.2$ to 7.5 km. Strong motion durations for the general records range from 10 to 30 seconds and from 3 to 10 seconds for the near-fault records. For multi-hazard analyses, it is assumed that the acceleration component of the records can be linearly scaled based on the spectral acceleration computed at the fundamental period of the structure, $S_a(T_1)$. Shome and Cornell (1999) have demonstrated that, compared to other approaches, scaling based on $S_a(T_1)$ will reduce the record-to-record dispersion in the response data and will not bias the results. An example set of results for the 6-story RCS frame subjected to the bin of near-fault records is shown in Fig. 4. Here the spectral accelerations of the scaled earthquake records $S_a(T_1)$ are related to the maximum inter-story drift ratio, IDR, from corresponding time-history analyses. Thus, each point in Fig. 4 corresponds to the peak response from a single time history, and the eight plots joining the points for each record are referred to as Incremented Dynamic Analyses (IDA).

One can observe from the near-fault IDA in Fig. 4 that the results tend to fall into two groups, a lower and upper set, where the lower set is more damaging with higher IDR for smaller S_a . Examination of the records reveals that those in the lower group have a pulse period, T_p , that is larger than the first mode period T_1 of the structure. For example, ground motions corresponding to the four lower curves have ratios of $T_p/T_1 = 1.8$ to 2.7 , whereas those for the upper curves have ratios of $T_p/T_1 = 0.7$ to 1.0 . Here “pulse period” is defined by the peak in the velocity spectra of the records. The resulting behavior is explained by the notion that when $T_p/T_1 > 1.0$ the structure softens into the more damaging pulse energy of the earthquake whereas in the other case, i.e. $T_p/T_1 < 1.0$, the opposite occurs. Differences of this sort indicate that an improved intensity scaling technique should involve both $S_a(T_1)$ and a second index that reflects the frequency content of the record, as might be reflected by the velocity spectra.

Frame stability limit state determination

Owing to the limitations of the time history analyses to fully capture the actual strength and stiffness degradation in the structure, the IDA results (Fig. 4) do not in themselves provide a definitive means of establishing a

stability (or *near-collapse*) limit of the structure. This is evident from the fact that some of the response curves in Fig. 4 continue to have a positive slope at very large S_a and IDR. While the damage index introduced earlier can characterize localized conditions, one still needs a means of integrating the local damage indices to understand their effect on overall structural stability. To address the question of global stability, a multi-step procedure is developed to post process the time history analysis with a *gravity load stability analysis* that accounts for the distribution of damage that develops during each time history analysis. This procedure entails the following steps (Mehanny 1999):

1. Perform a nonlinear time-history analysis and calculate the cumulative damage indices per Eq. 1. This provides the basis to quantify the localized (distributed) damage following an earthquake.
2. Modify the analysis model based on the damage incurred during the time-history analysis. Specifically, this involves reducing element stiffnesses and strengths as a function of the cumulative damage indices and incorporating the residual (permanent) building drift into the structural topology.
3. Reanalyze the modified structural model through a second-order inelastic static analysis under gravity loads up to the point of reaching an inelastic stability limit. The resulting gravity load stability index, λ_u , is defined as the ratio of the vertical gravity load capacity to the unfactored gravity loads.

The index, λ_u , thus serves as a global criterion that rationally integrates the destabilizing effects of local damage and residual drifts, thus avoiding the need for more ad-hoc averaging techniques sometimes employed to relate local indices to global response. Fig. 5 shows the evolution of damage from the undamaged state, $\lambda_u = \lambda_{uo}$, to incipient collapse at $\lambda_u = 1.0$ for the eight near-fault records. The large initial stability index, $\lambda_{uo} = 5.5$, is a function of the structure being designed for high seismic forces. Each point in Fig. 5 results from an independent time-history analysis and relates to a corresponding point in Fig. 4. These data can be used, for example, to relate stability performance limits to seismic hazard (intensity) levels.

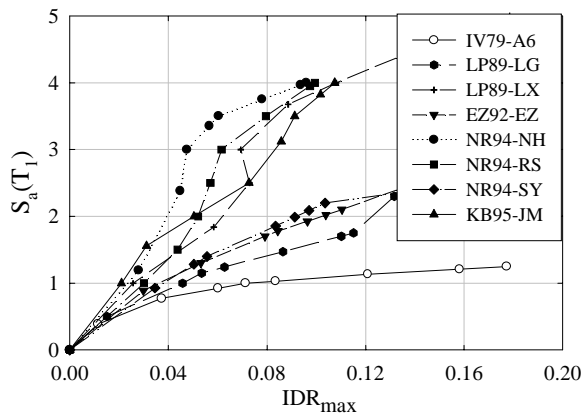


Figure 4. S_a -IDR_{max} relationship for near-fault records.

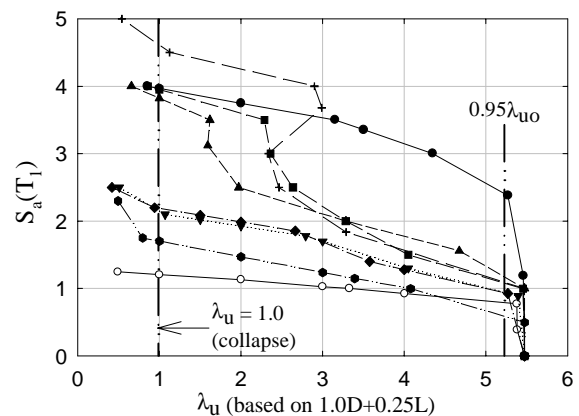


Figure 5. S_a - λ_u relationship for near-fault records.

By definition, the stability criterion of $\lambda_u \leq 1.0$ describes a state of collapse (or *near collapse*) when the structure can no longer support its gravity load. Another limit state that can be identified in Fig. 5 is the point at which the lateral stability begins to significantly degrade. Here we have defined this limit at $\lambda_u = 0.95\lambda_{uo}$, which, as shown in Fig. 5, occurs where there is a sharp transition in the stability curve. One might consider these two limit states, $\lambda_u = 0.95\lambda_{uo}$ and $\lambda_u = 1.0$, as corresponding to the “life safety” and “near-collapse” performance levels envisioned in such documents as FEMA 273. This may imply, for example, that at $\lambda_u = 0.95\lambda_{uo}$ the IDR should be close to the drift index of 2.5% that FEMA 273 suggests as representative of *Life Safety* performance.

Summary assessment of 6-story composite RCS and steel moment frames

Summarized in Table 2 are statistical response quantities for the two limit states ($\lambda_u = 0.95\lambda_{uo}$ and $\lambda_u = 1.0$) of the RCS and steel moment frames subjected to the two sets of ground records. Coefficients of variation (COV) for S_a are determined assuming that the data are normally distributed. These summary data are derived, for each frame and loading condition, from plots similar to those shown in Figs. 4 and 5. So as to minimize dispersion due to systematic effects associated with pulse periods in the near-fault records, statistics for the near-fault analyses are distinguished between records with $T_p/T_1 < 1$ and $T_p/T_1 > 1$.

Table 2 Summary of seismic stability performance indices

Frame	Records	$\lambda_u = 0.95\lambda_{uo}$			$\lambda_u = 1.0$		
		Sa (mean)	Sa (COV)	IDR	Sa (mean)	Sa (COV)	IDR
RCS	NF: Tp/T1 > 1	0.82 g	20 %	0.034	1.83 g	26 %	0.11
	NF: Tp/T1 < 1	1.44 g	44 %	0.033	4.05 g	9 %	0.10
	General	1.45 g	32 %	0.036	3.09 g	37 %	0.08
STEEL	NF: Tp/T1 > 1	0.85 g	16 %	0.034	2.39 g	28 %	0.11
	NF: Tp/T1 < 1	1.30 g	24 %	0.032	4.59 g	9 %	0.10
	General	1.30 g	18 %	0.035	3.82 g	36 %	0.08

Presuming that the limits $\lambda_u=0.95\lambda_{uo}$ and $\lambda_u=1.0$ do correspond to performance levels of “near-collapse” and “life safety”, the following observations can be drawn from the data in Table 2:

- Drift versus stability criterion:* Overall, the maximum IDRs for the two frames subjected to various ground motions are remarkably consistent. At $\lambda_u = 0.95\lambda_{uo}$ the average IDRs range between 3% to 3.5%, and there are no perceptible differences between drifts for the different ground motion bins. The range of 3% to 3.5% is slightly larger than the value of 2.5% suggested by FEMA 273 for life safety and, referring to the pushover results in Fig. 3, is about twice the drift where the response curve deviates from linearity. At $\lambda_u=1.0$, there are consistent differences between response for the general and near-fault records, where IDR = 10 to 11% for the near-fault records and IDR = 8% for the general records. The smaller IDR for the general records is probably due to their longer strong motion duration that leads to larger cumulative damage and stiffness/strength degradation, which in turn causes the stability limit to be reached at smaller drift ratios.
- Relating $\lambda_u = 0.95\lambda_{uo}$ to $\lambda_u=1.0$:* Ratios of S_a at $\lambda_u=0.95\lambda_{uo}$ (life safety) versus $\lambda_u=1.0$ (near collapse) range from $S_a(\lambda_u=1.0)/S_a(0.95\lambda_{uo}) = 2.1$ to 2.8 for the RCS frame and 2.8 to 3.4 for the steel frame. The ratios are slightly larger for the steel frame, perhaps because the steel damage indices do not degrade as rapidly under cyclic loading as those for reinforced concrete. Both sets of ratios indicate that the hazard intensity for near collapse ($\lambda_u=1.0$) is over twice that corresponding to the point when the structure begins to significantly degrade ($\lambda_u=0.95\lambda_{uo}$). This margin is larger than the ratio of 1.5 implied by modern codes between the “design level” earthquake response (geared to life safety) and the maximum considered earthquake (geared to near collapse).
- Relating performance to hazard levels:* While a clear consensus has yet to emerge on linking structural performance to seismic hazard levels, documents such as the IBC 2000 and FEMA 273 suggest that buildings should exceed near-collapse performance for a 2% in 50 year hazard and life safety performance for the design earthquake, nominally a 10% in 50 year hazard. For the case study buildings, the 2% in 50 year hazard is characterized by spectral acceleration of $S_a(2\%in50) = 0.86g$, and assuming that the 10% in 50 year hazard is about 2/3 of this, $S_a(10\%in50) = 0.57g$. Comparing these to the mean values of $S_a(\lambda_u=1.0)$ and $S_a(0.95\lambda_{uo})$ in Table 2, both the RCS and steel buildings exceed the minimum requirements by a reasonable margin – due in large part to their high overstrength. In the most severe case - the RCS frame subjected to damaging near-field pulse motions - the performance/hazard ratios are $S_a(\lambda_u=1.0)/S_a(2\%in50) = 2.1$ and $S_a(\lambda_u=0.95\lambda_{uo})/S_a(10\%in50) = 1.4$. For the RCS frame subjected to the general records, the ratios are $S_a(\lambda_u=1.0)/S_a(2\%in50) = 3.6$ and $S_a(\lambda_u=0.95\lambda_{uo})/S_a(10\%in50) = 2.5$. Critical spectral acceleration values for the steel frame are about the same as those in the RCS frame at the $\lambda_u=0.95\lambda_{uo}$ level and about 15% larger at the $\lambda_u=1.0$ level.
- Variability of Response:* Given the rather large variability in spectral performance levels, as reflected by the $S_a(COV)$ in Table 2, one may consider relating performance levels to seismic hazards by comparing *mean minus standard deviation* levels – rather than *mean* levels. Accordingly, for the most critical case of the RCS frame under near-fault motions, performance/hazard ratios reduce to $S_a(\lambda_u=1.0)/S_a(2\%in50) = 1.6$ and $S_a(\lambda_u=0.95\lambda_{uo})/S_a(10\%in50) = 1.2$, and ratios for the general records reduce to 2.3 and 1.7, respectively. These ratios still exceed unity in all cases, indicating that the frame would exceed the desired performance at the 10% and 2% in 50 year hazard levels.

RESPONSE DEPENDENCY ON GROUND MOTION PARAMETERS

Data given in Figs. 4 and 5 and Table 2 relate global response measures (IDR or λ_u) to the single intensity parameter, $S_a(T1)$. Shown in the second row (S_a) of Table 3 are results of a regression analysis of this data for the RCS frame using a power law model. The regression is linear in the log-log space and applied to the response parameters (IDR or λ_u) conditioned on the input intensity $S_a(T1)$. The power equations in Table 3 relating S_a to IDR and λ_u represent median curves for the data shown in Figs. 4 and 5. The statistical indices, conditional dispersion, σ , and adjusted coefficient of determination, R_a^2 , are also given. Values of $R_a^2 = 0.26$ to 0.40 and $\sigma = 0.45$ to 0.62 for the regression to $S_a(T1)$ suggest that there is room for improvement to improve the correlation. Note that the range of R_a^2 is 0 to 1, with $R_a^2 = 1.0$ implying the strongest possible correlation with perfect agreement between the data and regression.

Table 3 Regression equations for RCS frame response to near-field records

Index	Maximum Interstory Drift Ratio (IDRmax)	Stability Index (λ_u)
S_a	$\text{IDR}_{\max} = 0.046 S_{a_1}^{0.64}$ $\sigma_{\ln \text{IDR}_{\max} S_{a_1}} = 0.45 \quad R_a^2 = 0.40$	$\lambda_u = 3.47 S_{a_1}^{-0.72}$ $\sigma_{\ln \lambda_u S_{a_1}} = 0.62 \quad R_a^2 = 0.26$
$S_a \ \& \ R_{S_a}$	$\text{IDR}_{\max} = 0.064 S_{a_1}^{1.26} R_{S_a}^{1.14}$ $\sigma_{\ln \text{IDR}_{\max} S_{a_1}, R_{S_a}} = 0.22 \quad R_a^2 = 0.86$	$\lambda_u = 2.55 S_{a_1}^{-1.62} R_{S_a}^{-1.43}$ $\sigma_{\ln \lambda_u S_{a_1}, R_{S_a}} = 0.43 \quad R_a^2 = 0.65$

Among the possible additional input parameters to reduce the conditional dispersion is the ratio R_{S_a} which reflects the *shape* of the ground acceleration response spectrum in the vicinity of T1. R_{S_a} is defined as the ratio of the spectral acceleration at a longer period, Tf, representing a *decrease of lateral stiffness* due to earthquake induced damage, to the spectral acceleration at the fundamental elastic period, T1. Tf is calculated as the period associated with a secant lateral stiffness derived from the pushover analysis using a target displacement beyond yield. Using the target displacement formula proposed by FEMA 273, we calculated Tf = 2.2 seconds for the 6-story RCS frame, roughly twice the initial value of T1=1.25 seconds. Equations relating R_{S_a} and $S_a(T1, \xi=5\%)$ to the response quantities are given in the bottom row of Table 3, where the decrease in dispersion, σ , and increase in R_{S_a} indicates an improved correlation with the data. The net effect is that uncertainty in the estimation of median IDRmax with a limited sample size of eight records is cut in half from 16% ($=0.45/\sqrt{8}$) to 8% ($=0.22/\sqrt{8}$), and uncertainty in the estimation of λ_u reduces from 22% to 15%. For general records, not shown here, corresponding drops are from 15% to 10% and from 21% to 16% for IDRmax and λ_u , respectively.

We are currently investigating other parameters to further improve the correlation of ground motion to response, including as possible candidates the strong motion duration and near-fault pulse periods. However, no definite conclusions have yet be made, in part because of the narrow range of strong motion durations and pulse period values in the bins of ground records used for our analyses. Further, distinctions based on magnitude and distance (M-R) are beyond the scope of this research, although Shome and Cornell (1999) have previously shown that the response of non-degrading structures has only a *mild* dependency on M-R, provided that the ground records used for the hazard analysis generally represent the M-R hazard conditions at the site.

Based on our analyses, we can suggest that a dual earthquake intensity index of $S_a(T1, \xi=5\%)$ and R_{S_a} would be effective for reducing the record-to-record dispersion of the response. This would in turn reduce the standard error of estimation of the median response and decrease the number of nonlinear time history analyses needed to achieve a certain confidence level. The main disadvantage of this dual index is that current hazard maps only report $S_a(T1, \xi=5\%)$ and do not distinguish hazards on the basis of R_{S_a} . It would be worthwhile, to confirm whether the promising results shown here using the two terms $S_a(T1, \xi=5\%)$ and R_{S_a} apply for other types of records and other structures. If so, then this would suggest a direction for improving seismic hazard maps by adding this sort of information for engineers to include in seismic hazard analyses.

CONCLUSIONS

The nonlinear analyses presented in this paper demonstrate satisfactory seismic performance of composite RCS framed structures when evaluated relative to performance levels implied by codes and in comparison with steel frames. This conclusion is, however, limited to the six-story trial design studies examined in this paper where the static overstrength was fairly large and redundant space frames were used. Additional case studies would be an obvious topic of future work. A newly proposed technique, which integrates the local damage effects with system stability analysis, offers a reliable tool to quantify “near-collapse” performance. It further provides insight to relate the degradation of global stability to performance and hazard levels suggested by seismic codes. The paper also suggests approaches to reduce the variability observed in nonlinear time history analyses by considering additional ground motion parameters beyond $S_a(T_1)$. For example, when used in conjunction with scaling to $S_a(T_1)$ the ratio of $R_{S_a} = S_a(T_f) / S_a(T_1)$ significantly reduces the dispersion. Near-fault records with pulse periods greater than the building period, $T_p/T_1 > 1$, are shown to be significantly more damaging than near-fault records with $T_p/T_1 < 1$ or general records without forward directivity effects.

ACKNOWLEDGEMENTS

Financial support of the National Science Foundation (CMS-9632502) and the Nippon Steel Corporation is gratefully acknowledged. The authors also acknowledge the advice of C.A. Cornell of Stanford University regarding the seismic hazard analyses and contributions to the authors’ research on RCS structures by R. Kanno, S. El-Tawil, H. Kuramoto, and P. Cordova.

REFERENCES

- American Institute of Steel Construction, Inc., “Seismic Provisions for Structural Steel Buildings,” 2nd Edition, Chicago, Illinois, April, 1997.
- ASCE Guidelines (1994), “Guidelines for Design of Joints Between Steel Beams and Reinforced Concrete Columns,” *Journal of Structural Division, ASCE*, Vol. 120(8), pp. 2330-2357.
- El-Tawil, S., and Deierlein, G.G. (1996a), "Inelastic Dynamic Analysis of Mixed Steel-Concrete Space Frames," *Struct. Engrg. Report 96-5*, Cornell Univ., Ithaca, NY, 235 pgs.
- El-Tawil, S., Kanno, R., and Deierlein, G.G. (1996b), "Inelastic Models for Composite Moment Connections in RCS Frames," *Proc. of Composite Constr. III*, ASCE, NY, pp. 197-210.
- Griffis, L.G. (1992), "Composite Frame Construction," *Constructional Steel Design - An International Guide*, Ed. Dowling et al., Elsevier Applied Science, NY, pp. 523-554.
- IBC 2000 (1998), “International Building Code,” *Inter. Code Council*, Falls Church, VA, Final Draft, July, 1998.
- Kanno, R., and Deierlein, G.G. (1996), "Seismic Behavior of Composite (RCS) Beam-Column Joint Subassemblies," *Proc. of Composite Constr. III*, ASCE, NY, pp. 236-249.
- Mehanny, S.S.F. (1999), “Modeling and Assessment of Seismic Performance of Composite Moment Frames with Reinforced Concrete Columns and Steel Beams,” *Ph.D. Thesis*, Stanford University, Stanford, CA.
- Shome, N., and Cornell, C.A. (1999), “Probabilistic Seismic Demand Analysis of Nonlinear Structures,” *Report No. RMS-35*, Stanford University, Stanford, CA, 320 pgs.